Available online at www.sciencedirect.com
SCIENCE DIRECT®
Journal of Power Sources 143 (2005) 67–74
JOURNAL OF POWER SOURCES
www.elsevier.com/locate/jpowsour

Magnetotomography—a new method for analysing fuel cell performance and quality

Karl-Heinz Hauer[a,*], Roland Potthast[b], Thorsten Wüster[c], Detlef Stolten[d]

[a] *TomoScience GbR, Major-Hirst-Strasse 11, 38442 Wolfsburg, Germany*
[b] *Universität Göttingen, NAM, Lotzestrasse 16-18, 37083 Göttingen, Germany*
[c] *Chair for fuel cells, RWTH Aachen, 52056 Aachen, Germany*
[d] *Forschungszentrum Juelich GmbH, 52425 Juelich, Germany*

Received 30 August 2004; received in revised form 9 November 2004; accepted 15 November 2004
Available online 21 January 2005

Abstract

Magnetotomography is a new method for the measurement and analysis of the current density distribution of fuel cells. The method is based on the measurement of the magnetic flux surrounding the fuel cell stack caused by the current inside the stack. As it is non-invasive, magnetotomography overcomes the shortcomings of traditional methods for the determination of current density in fuel cells [J. Stumper, S.A. Campell, D.P. Wilkinson, M.C. Johnson, M. Davis, In situ methods for the determination of current distributions in PEM fuel cells, Electrochem. Acta 43 (1998) 3773; S.J.C. Cleghorn, C.R. Derouin, M.S. Wilson, S. Gottesfeld, A printed circuit board approach to measuring current distribution in a fuel cell, J. Appl. Electrochem. 28 (1998) 663; Ch. Wieser, A. Helmbold, E. Gülzow, A new technique for two-dimensional current distribution measurements in electro-chemical cells, J. Appl. Electrochem. 30 (2000) 803; Grinzinger, Methoden zur Ortsaufgelösten Strommessung in Polymer Elektrolyt Brennstoffzellen, Diploma thesis, TU-München, 2003; Y.-G. Yoon, W.-Y. Lee, T.-H. Yang, G.-G. Park, C.-S. Kim, Current distribution in a single cell of PEMFC, J. Power Sources 118 (2003) 193–199; M.M. Mench, C.Y. Wang, An in situ method for determination of current distribution in PEM fuel cells applied to a direct methanol fuel cell, J. Electrochem. Soc. 150 (2003) A79–A85; S. Schönbauer, T. Kaz, H. Sander, E. Gülzow, Segmented bipolar plate for the determination of current distribution in polymer electrolyte fuel cells, in: Proceedings of the Second European PEMFC Forum, vol. 1, Lucerne/Switzerland, 2003, pp. 231–237; G. Bender, S.W. Mahlon, T.A. Zawodzinski, Further refinements in the segmented cell approach to diagnosing performance in polymer electrolyte fuel cells, J. Power Sources 123 (2003) 163–171]. After several years of research a complete prototype system is now available for research on single cells and stacks.

This paper describes the basic system (fundamentals, hardware and software) as well as the state of development until December 2003. Initial findings on a full-size single cell will be presented together with an outlook on the planned next steps.

Keywords: Fuel cells; Magnetotomography; Current density distribution

1. Introduction

Many factors such as temperature, reactant humidity, partial pressures of feed gases and flow field structure in combination with the membrane electrode assembly (MEA) affect the current density distribution and with this the performance of a proton exchange fuel cell (PEFC). Several methods for the measurement of the current density distribution are known and have been discussed in the literature [1–8]. The disadvantages of these methods are that they are invasive, inflexible and also that the feedback effect on the measured current density distribution is unclear.

Magnetotomography [11] allows the non-invasive measurement and 3D-visualisation of the current density distribution of single fuel cells and fuel cell stacks. The method is

* Corresponding author.
E-mail address: hauer.@tomoscience.com (K.-H. Hauer).

0378-7753/$ – see front matter © 2004 Elsevier B.V. All rights reserved.
doi:10.1016/j.jpowsour.2004.11.054

based on the measurement of the magnetic flux surrounding the fuel cell stack caused by the current inside the stack. The magnetic flux data are measured with a 3D magnetic flux sensor. In order to sense the necessary magnetic flux data at different positions relative to the test object (cell, stack) a four-axis positioning system was developed. Magnetic field data and sensor position together allow the current flow inside the cell to be calculated. The relation between magnetic field data and the current density is generally described by a Maxwell equation Eq. (1). For the special problem of the current density of a fuel cell the Biot–Savart law was applied. The image quality of the calculated current density depends on the measurement error, the number and position of data points taken and the algorithm applied in combination with additional boundary conditions.

2. Fundamentals

In this section, the applied fundamentals for the calculation of the current density based on magnetic flux data are explained. For ease of understanding the problem discussed in this paper is limited to a two-dimensional problem. In the prototype system, the full 3D algorithm was applied considering as input data 3D magnetic flux data (B_x, B_y, B_z) and calculating as output 3D current densities (J_x, J_y, J_z).

The magnetic field outside an operating fuel cell is measured at a number of locations close to the fuel cell. Based on this data and the position of the data points relative to the fuel cell, the current density distribution inside the fuel cell is calculated.

The following section explains the calculation of a single unknown current (a current flowing in a thin, infinite long wire) based on field data surrounding this current and generated by the current.

The relation between the current density J and the magnetic field H (Fig. 1) is defined by the Maxwell equation Eq. (1):

$$\oint_{\text{Boundary of } A} \vec{H}\,\mathrm{d}\vec{s} = \iint_{A} \vec{J}\,\mathrm{d}\vec{A} \tag{1}$$

For the case of a single infinitely thin and infinitely long wire it follows from Eq. (1) that the magnetic field H is a function of the distance from the centre of the wire Eq. (2). In Eq. (2), I represents the total current flowing in the wire.

$$H 2\pi r = I \tag{2}$$

The sensors used in the prototype equipment do not measure the magnetic field strength H but the magnetic flux B. In air, the magnetic flux B is directly proportional to the magnetic field strength H (Eq. (3)).

$$B = \mu_0 H \tag{3}$$

The factor μ_0 is the magnetic permeability of the vacuum. The magnetic permeability of almost all materials used in significant quantities in fuel cells is very close to the magnetic permeability of the vacuum. The only exception is magnetic steel and iron. For the application of magnetotomography these materials have to be substituted with other materials with a permeability close to μ_0, e.g. aluminium or non-magnetic steel.

For the case of non-concentrated volume-distributed currents as in a real fuel cell, the resulting magnetic field outside the cell can be derived by superposition of the magnetic fields of a number of discrete currents. Fig. 2 illustrates the discretisation of a cell surface in a total of 36 segments. Each of these segments carries an unknown current flowing through the geometric centre. The sum of the 36 currents represents the total cell current which is known and which can be measured at the cell terminals. According to our problem, we now want to calculate the 36 unknown currents solely from the measured magnetic flux data outside the stack.

$$\begin{aligned}
H^i_{x,j} &= \frac{I_i}{2\pi\sqrt{\Delta x^2 + \Delta y^2}} \sin\left(\operatorname{atan}\frac{\Delta y_{i,j}}{\Delta x_{i,j}}\right) \\
H^i_{y,j} &= \frac{I_i}{2\pi\sqrt{\Delta x^2 + \Delta y^2}} \cos\left(\operatorname{atan}\frac{\Delta y_{i,j}}{\Delta x_{i,j}}\right) \\
H_{x,j} &= \sum_i H^i_{x,j} \\
H_{y,j} &= \sum_i H^i_{y,j}
\end{aligned} \tag{4}$$

where i is the index for the 36 unknown currents and j is the index for the measurement points (at least 18).

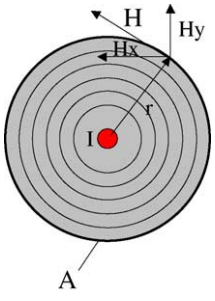

Fig. 1. Magnetic field and current for the case of an infinitely long wire.

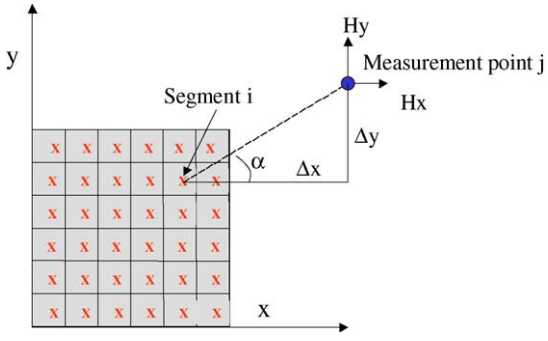

Fig. 2. Discrete cell surface (6 × 6 segments).

Eq. (4) describes the calculation of the magnetic field strength H_x und H_y at the measurement point j as a function of the (in our example 36) unknown currents I_i (for $i = 1, \ldots, 36$). For the calculation of the 36 unknown currents based on magnetic field data at least 36 measurement values are required. Since our assumed sensor is able to measure not only the absolute field strength at each position but can separate the x and y components we need to take measurements at (at least) 18 different locations (18 H_x values und 18 H_y values).

In matrix form the relation between magnetic field strength and unknown currents can be stated as in Eq. (5). In Eq. (5), it has been assumed that all of the 36 required field values are H_x components, which are taken at 36 different locations around the fuel cell.

$$\begin{pmatrix} H_{x,1} \\ \vdots \\ H_{x,n} \end{pmatrix} = \begin{bmatrix} a_{1,1} & \cdots & a_{1,m} \\ \vdots & & \vdots \\ a_{n,1} & \cdots & a_{n,m} \end{bmatrix} \begin{pmatrix} I_1 \\ I_2 \\ \vdots \\ I_i \\ \vdots \\ I_m \end{pmatrix} \tag{5}$$

The matrix (A) in Eq. (5) with its elements $a_{i,j}$ is of the size 36×36. It includes the geometric data connecting the current vector I and the field vector H. The inversion of Eq. (5) provides the 36 unknown currents I for the known field distribution H. However, the nature of the problem leads to a so-called ill-conditioned matrix A. The trivial matrix inversion would lead to significant errors for the unknown currents I if the measurement data are not mathematically exact, which is always the case with real measured data. In practice, the result of the simple matrix inversion would lead to totally unusable results for I as soon as the H values have the smallest error.

Therefore, the matrix needs to be regulated[1] and we apply a Tikhonov regularisation to extract information about the currents from the equation system. As a consequence of the regularisation, the exact determination of the current density distribution is not possible but we can obtain technical valuable information even with standard sensors and a large error margin in the field data as discussed in results section.

The error between calculated currents and real currents is a function of:

1. The positioning of the magnetic field measurement points relative to the test object (fuel cell).
2. The measurement error included in the acquired magnetic field data.
3. The discretisation of the volume of interest (model).[2]
4. The mathematical algorithm applied for the matrix inversion (regularisation).
5. Applied additional boundary conditions.

Each of the items listed above has a significant influence on the resulting current vector I. Only if all of the steps are handled with great care can one expect technically valuable information about the current density distribution inside the cell.

It should be noted that the real problem is not of a two-dimensional nature with currents flowing in just one direction, as assumed in the example, but of a three-dimensional nature with currents flowing in all three directions. In addition to the current flow through the membrane, lateral currents flowing in the bipolar plates influencing the magnetic field outside the stack need to be considered. The outside field vectors therefore have three components, H_x, H_y and H_z, of interest for a realistic calculation of the current flow inside the cell. This fact complicates the problem but does not change it in principle. More of the mathematical background and the complete 3D-problem is provided in [9,10,12].

3. Hardware

Two sensors are used for magnetic field data acquisition. The first sensor scans the top layer, left and right side and front and rear side (if accessible) of the cell. The second sensor scans the bottom layer of the fuel cell. For the position of the sensors around the fuel cell surface, a four-axis positioning system is developed (Fig. 3). The control software of the four axes runs on a personal computer (PC) and is programmed in Labview. The software communicates with the four motion controllers, one for each axis, sending set points to each controller. In addition to the motion control, the software controls the data acquisition at each location. If one sensor arrives at its target location the sensor is initialised and after initialisation the data are taken, converted into a digital format, filtered and stored together with the sensor position in a data file. After a complete scan this data file contains a list of sensor positions together with the magnetic field data at each position.

The sensor data are listed in Table 1. The sensors are off-the-shelf products that are not specifically designed for this application.

4. Software

Two main software modules are necessary:

- "XcellMeasure" for data acquisition and

[1] While regularisation of the matrix conserves the relationship between magnetic field data and the searched current density distribution it reduces the influence of the in the field data contained measurement errors. Compared to the current distribution gained with an unregulated or only little regulated matrix the process of regulation leads to a smoothed out current density distribution.

[2] The real current density is continuous. However, the Magnetom method approximates the continuous current density distribution with discrete currents flowing in a three-dimensional grid. The transition from the continuum to the discrete grid model introduces an error. In addition the grid characteristics (size, geometry, ...) influences the error margin.

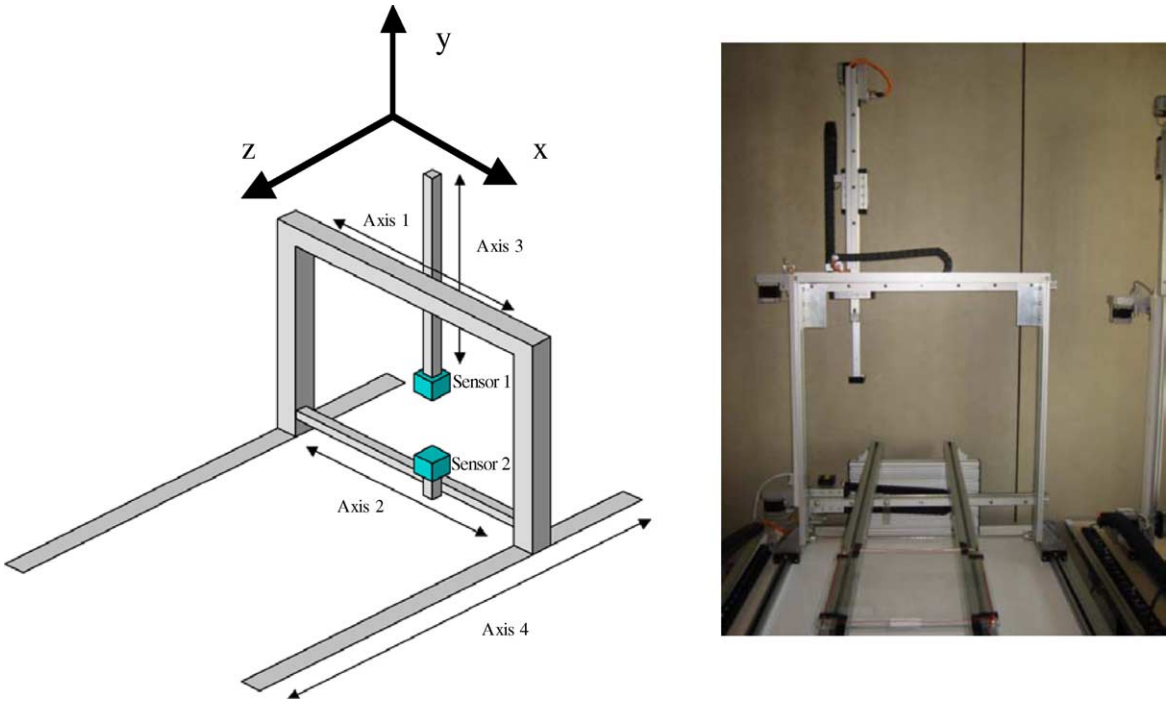

Fig. 3. Positioning system and the location of the sensors. The physical dimensions are $L = 1.6$ m, $W = 1$ m, $H = 2$ m.

Table 1
Sensor specification

	Value	Comment
Linearity error	±1%	
Range	−2 bis + 2 G	Compare with earth magnitc field 0.3, . . ., 0.6 G
Magnetic field resolution	40 μ G	50.000 increments
Repeatability	0.05%	
Dynamic	>100 Hz	
Measurement of all three vector components	Yes	

- "Magnetom" for the calculation and visualisation of the current density based on the scanned magnetic field data.

4.1. "XcellMeasure" data acquisition software

The software module for the data acquisition is written in Labview. XcellMeasure controls the positioning of the sensors and the scanning of the field data after a sensor has arrived at its designated position. The maximum number of data points is not limited. In practice, several times as many data points as required are scanned to calculate the unknown current densities. The discretisation of the surface of a single cell into 36 segments and the description of the current density of each cell with three components, J_x, J_y and J_z, leads to a total of 108 unknown current density components. If all three components of the magnetic flux in each measurement point are scanned a minimum of 36 locations resulting in 108 flux values are needed. However, the scans are normally performed at more than 100 locations and therefore the equation system has more than 300 equations for the unknown 108 currents. The filter algorithm applied in the software contains redundant information and provides the solution for the unknown currents. The definition of the locations for the measurement points depends on the geometric situation. Areas occupied by cables, tubes and the fuel cell itself are not accessible and need to be left out of the input file containing the locations of the desired scan points.

4.2. "Magnetom" reconstruction and visualisation software

The Magnetom software takes as its input file the result file produced by the XcellMeasure software. This file contains the position and the magnetic flux values of each data point scanned. Based on this input data, the Magnetom software calculates the current density of the area inside the stack volume of interest. The Magnetom software also requires additional input information. An overview of the minimum required input information is given in Table 2.

Table 2
Input information required by the Magnetom software

Input required from Magnetom	Comment
Location of test object (cell, stack)	Cartesian coordinate system is defined
Size of the test object	Size of the cell or stack ($L \times W \times H$)
Discretisation	Discretisation of the volume of interest in all three dimensions, e.g. a $5 \times 5 \times 5$ discretisation defines 125 volumes. Each volume is characterized by three current densities (J_x, J_y, J_z)
Grid model applied	A choice can be made between several different grid models
Regularisation parameter	Since the solution of the equation system is not exact a regularisation parameter is required. Smaller positive regularisation parameters provide a more detailed image. However, a too small regularisation parameter leads to large errors (compare the function of the regularisation parameter with the dials of a binocular)
Reference file	Since we need to subtract the earth's magnetic field as well as the influence of the terminals a reference file is required

5. Initial results

The results presented in this section of the paper were obtained at Forschungszentrum Juelich (Germany) using a single cell equipped with an independent reference method for the measurement of the current density distribution (segmented shunt with a total of 20 segments). The cell data and the operating parameters are listed in Table 3. The geometry of the cell and the location of gas inlets, outlets and cooling are shown in Fig. 4. The measurements were made in a standard laboratory environment.

Since we made differential measurements no special shielding of the earth's magnetic field or other special precautions were necessary. A differential measurement consists of two scans. Scan 1 is a base scan with a base parameter set. For the second scan, an operating parameter (e.g. air flow, humidification, etc.) is changed.

$$\begin{aligned} B_1 &= B_{\text{earth}} + B_{\text{cable}} + B_{\text{cell1}} \\ B_2 &= B_{\text{earth}} + B_{\text{cable}} + B_{\text{cell2}} \\ B_{\text{diff}} &= B_2 - B_1 = B_{\text{cell1}} - B_{\text{cell2}} \end{aligned} \tag{6}$$

The difference between the two scans indicates the change in current density within the cell due to the change of the operating parameter. As Eq. (6) shows, the influence of the earth's magnetic field and the cable are not part of the difference B_{diff} in the measured magnetic fields B_1 and B_2. The difference in the magnetic field is used for the calculation of the differences in current densities. Each data scan requires approximately 15 min. The reconstruction of the current density data takes about 1 min on a standard 1 GHz PC.

6. Discussion

Figs. 5–7 show the influence on the current density distribution[3] for the change of an operating parameter (relative H_2 humidity or the stoichiometric ratio on the air side λ). All other operating parameters stayed unchanged. The influence was measured by two different and independent methods, a segmented shunt approach and the new magnetotomographic method introduced here. Both methods show similar trends (Figs. 5 and 6).

Fig. 5 shows the impact on current density through the reduction of H_2 humidity from a relative humidity of 100 to 15%. The blue areas indicate a reduction in current density while the red areas indicate an increase in current density. The change could be explained by a less active reaction due to a lack of water directly at the stack inlet. Because of the constant total current (73.3 A), the current density has to increase in other regions of the cell (red areas).

It should be noted that both methods do not measure exactly the same current density and are therefore not 100% comparable. The segmented shunt approach measures the current density in a segmented plane added to the cell (membrane, backing layer and bipolar plates are not segmented). Because of possible lateral currents in the backing layer and the bipolar plate the current density measured with this approach is not 100% identical with the current density flowing through the membrane.

On the other hand the Magnetom method is sensitive to the complete current streamlines in the control volume. Since the dimensions of the discretized volumes exceed the membrane thickness, the current density indicated for the volumes containing the membrane represents an average of the current density in the membrane, the backing layer and the bipolar plates.

Fig. 6 shows the effect of an increase in air stoic ratio from $\lambda_{\text{Air}} = 2$ to 4. Again the blue areas indicate a drop in current density while the red areas indicate an increase. While the current density decreases in the upper half of the cell, the lower half of the cell shows an increase in current density. This effect is expected since in the lower half of the cell the effects of oxygen depletion are reduced due to the increase in the stoichiometric ratio. Therefore, the reaction in this area close to the cathode exit is intensified and because of the total constant stack current the current density has to drop in other areas of the cell.

Fig. 7 shows the effects on current density distribution for a transition from operation with air ($\lambda_{\text{Air}} = 2$) to operation with pure oxygen ($\lambda_{O_2} = 2$). The effects are similar to the

[3] The expression current density refers to the component of the current density vector normal to the membrane. Only this vector is displayed in the figures shown in this paper. The other two current density components are also calculated but not discussed in this paper.

Table 3
Cell data and reference operating parameters

Parameter	Value
Active cell area [cm^2]	244
Total cell current [A]	73.3
Cell dimensions [cm]	17.7 × 13.8
Operating parameters (reference set)	Air side stoic ratio: $\lambda_{Air} = 2$ Hydrogen side stoic ratio: $\lambda_{H_2} = 1.1$ Cell temperature: $T_{cell} = 67\,^{\circ}C$ Operating pressure: $p = 2$ bar H_2 humidity: $\gamma_{H_2} = 100\%$ @ gas inlet Air humidity: $\gamma_{Air} = 100\%$ @ gas inlet Temperature humidifier: $T_{humidifier} = 75\,^{\circ}C$
Special modifications	All parts of the cell made from magnetic steel were replaced by parts made from non-magnetic materials (aluminium or stainless steel)

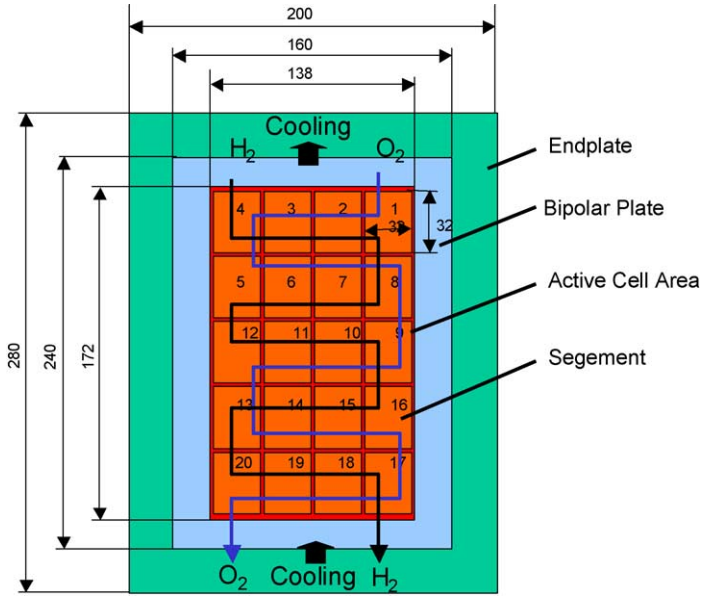

Fig. 4. Test cell with flow channels including the discretisation of the reference method for the current density distribution (5 × 4 segments).

effects observed in Fig. 6. Because of operation with pure oxygen the second half of the channel especially close to the exit no longer suffers any depletion of oxygen. Therefore, the reaction in this area close to the cathode exit is intensified and because of the total constant stack current in other areas of the cell the current density has to drop.

Fig. 7 does not shows the effect measured by the segmented shunt approach. This is because of technical problems with this reference method at the time the experiment was set up.

Comparing the results gained by the two methods for the measurement of the current density distribution, we observe the same trends but see still differences. We explain these differences with:

- The fact that although both methods measure the current density distribution in fuel cells, the measured current density is not taken at identical locations.

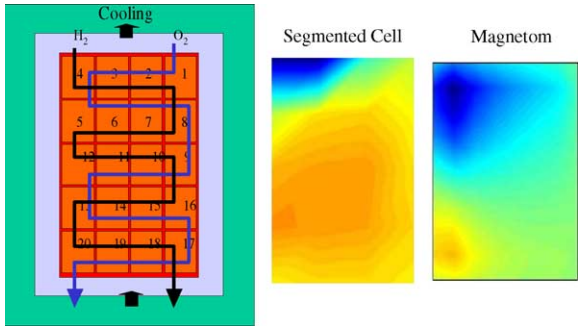

Fig. 5. Influence on the current density distribution of the reduction of H_2 relative humidity from 100 to 15% relative humidity. The middle column shows the component of the current density distribution normal to the membrane measured with the segmented shunt approach, the right column shows the same current density component measured by the Magnetom method.

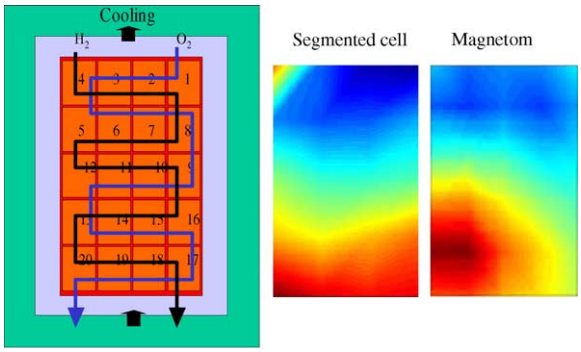

Fig. 6. Influence of the increase in air stoic ratio from $\lambda_{Air} = 2$ to 4.

- Both methods are still in a research phase meaning that error margins are still high and well above the short-medium term potential.

In addition to the validation on a single cell presented in this paper the principle of the Magnetom method has been very successfully verified with 3D-resistor networks in which the current distribution is exactly known.

For a more detailed validation on single cells we will repeat the experiments using a second different invasive and shunt based reference method. The results of this next step of validation will be presented later in this journal.

All of the results shown in this paper are based on differential measurements. The same equipment and software could also be used for absolute measurements in which we determine the absolute current density distribution and not the difference in current density distribution referenced to a base case. For absolute measurements we have to know the exact position of the connection wires since their influence is significant in absolute measurements.

With this information the cable influence can be corrected and absolute measurements can be made using the same hard and software as for the differential measurements. Experiments with absolute measurements will be performed in future.

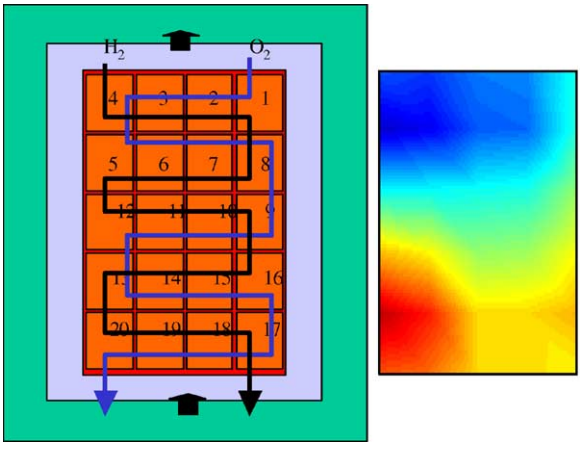

Fig. 7. Cathode oxygen changed from air ($\lambda_{Air} = 2$) to pure oxygen ($\lambda_{O_2} = 2$). The result was obtained by the Magnetom method. The reference method was not installed. The result compares very well with the results shown in Fig. 6. This similarity is expected.

The repeatability of the measurements is very good. This means that for an unchanged set of operating parameters two scans of the magnetic field provided the same current density distribution (meaning a change of almost zero over the complete cell area). This was also true even if there was a time span of several hours between the two scans.

The Magnetom software has not yet been calibrated. This means that we cannot say anything about the magnitude of the differences in current density shown in the figures above based solely on the Magnetom data. From analysing the data gained with the reference method the changes in current density are below 50 mA cm^{-2}. However, it is possible to calibrate the Magnetom method. One calibration method is the comparison with the data obtained by a reference method and the introduction of calibration factors. These calibration factors would be valid for all cells with the same geometry.

7. Summary and outlook

Magnetotomography is a new way of analysing the current density distribution in fuel cells. The advantage in comparison to conventional methods is that the method is non-invasive and that it has virtually no feedback effect on the test object and the current density distribution to be measured. The method is simple to apply, flexible and turns out to be reliable and practical in a standard laboratory environment. Apart from the research and development of fuel cells other application areas are the field of quality assurance in a production facility.

As yet, magnetotomography has only been tested on single cells. However, we believe that the method could also be applied to short stacks and even full size stacks if the accuracy of the magnetic flux measurement could be increased. Our next steps are the detailed characterisation of the current state of the technology, tests with absolute measurements, calibration of the equipment and an assessment of the technical feasibility of the technology.

Acknowledgements

Magnetotomography for fuel cells is based on a concept originally developed and patented[4] [13] by the company xcellvision (www.xcellvision.com) in 2001. Initial funding for the development of the method was provided by Wolfsburg AG, a public-private partnership of Volkswagen AG and the city of Wolfsburg. The results presented are obtained in close cooperation with the University of Goettingen Germany, Institute for Numerical and Applied

[4] The patent is owned by Volkswagen AG.

Mathematics and the German research center Forschungszentrum Juelich, Institut fuer Werkstoffe und Verfahren der Energietechnik—Energieverfahrenstechniken (IWV-3).

References

[1] J. Stumper, S.A. Campell, D.P. Wilkinson, C.M. Johnson, M. Davis, In situ methods for the determination of current distributions in PEM fuel cells, Electrochem. Acta 43 (1998) 3773.
[2] S.J.C. Cleghorn, C. R: Derouin, M.S. Wilson, S. Gottesfeld, A printed circuit board approach to measuring current distribution in a fuel cell, J. Appl. Electrochem. 28 (1998) 663.
[3] Ch. Wieser, A. Helmbold, E. Gülzow, A new technique for two-dimensional current distribution measurements in electro-chemical cells, J. Appl. Electrochem. 30 (2000) 803.
[4] Grinzinger, Methoden zur Ortsaufgelösten Strommessung in Polymer Elektrolyt Brennstoffzellen, Diploma thesis, TU-München, 2003.
[5] Y.-G. Yoon, W.-Y. Lee, T.-H. Yang, G.-G. Park, C.-S. Kim, Current distribution in a single cell of PEMFC, J. Power Sources 118 (2003) 193–199.
[6] M.M. Mench, C.Y. Wang, An in situ method for determination of current distribution in PEM fuel cells applied to a direct methanol fuel cell, J. Electrochem. Soc. 150 (2003) A79–A85.
[7] S. Schönbauer, T. Kaz, H. Sander, E. Gülzow, Segmented bipolar plate for the determination of current distribution in polymer electrolyte fuel cells, in: Proceedings of the Secondd European PEMFC Forum, vol. 1, Lucerne/Switzerland, 2003, pp. 231–237.
[8] G. Bender, S.W. Mahlon, T.A. Zawodzinski, Further refinements in the segmented cell approach to diagnosing performance in polymer electrolyte fuel cells, J. Power Sources 123 (2003) 163–171.
[9] R. Potthast, L. Kühn, On the convergence of the finite integration technique for the anisotropic boundary value problem of magnetic tomography, Math. Methods Appl. Sci. 26 (2003) 739–757.
[10] R. Kreß, L. Kühn, R. Potthast, The reconstruction of a current distribution from its magnetic fields, Inverse Problems 18 (2002) 1127–1146.
[11] K.H. Hauer Entwicklung eines bildgebenden Messsystems, das es erlaubt, die räumliche Stromdichteverteilung in Brennstoffzellen nichtinvasiv zu erfassen, VDE-Paper, Germany, 2001.
[12] R. Kreß, Linear integral equations, Applied Mathematical Sciences, vol. 82, Second ed., Springer-Verlag, Heidelberg, 1999.
[13] Patent “Method for determining the current density distribution in a fuel cell stack”, PCT 09154.